ANNUAL REPORT TO THE LASER FACILITY COMMITTEE 1991

5 April 1990 to 4 April 1991

SERC CENTRAL LASER FACILITY
RUTHERFORD APPLETON LABORATORY
CHILTON
DIDCOT
OXON
OX11 0QX

Telephone 0235 821900
Telefax 0235 445888

Rutherford Appleton Laboratory Report RAL-91-025

Cover designed by
J Houliston & J Mackintosh

MEASUREMENT AND ANALYSIS OF RADIATION TRANSPORT IN RADIATIVELY HEATED FOILS

J. Edwards, M. Dunne, L. Gizzi, O. Willi
Blackett Laboratory, Imperial College of Science, Technology and Medicine, London SW7 2BZ, U.K.

S.J. Rose
Rutherford Appleton Laboratory, Chilton, Didcot, Oxon. OX11 0QX U.K.

C.A. Back, C. Chenais-Popovics
Ecole Polytechnique, Laboratoire PMI, Palaiseau 91128, Cedex, France

1. Introduction

The importance of radiation transport both as a mechanism for the transfer of energy under certain laser and target conditions and for spectral analysis is well known and has been discussed in a number of articles (see for example 1-11). Here we present experimental measurements of radiation transport in thin plastic targets in which radiation transport is predicted to dominate the energy transfer. Planar foil targets were heated directly by soft X-rays emitted through the rear of a second laser heated high Z layer deposited on a thin plastic substrate. First, the soft X-ray emission from the rear of the high Z foil was investigated as a function of target design. Then a suitable target was used as a source of soft X-rays for heating a sample foil. The soft X-rays transmitted through the samples were measured using time resolved XUV spectroscopy in the 10-70A spectral wavelength region. The experimental conditions have been simulated with a 1D radiation hydrodynamics code and atomic physics data has been calclulated with a multi-configuration Dirac-Fock code for spectral analysis.

2. Experimental Arrangement

Six frequency doubled RPP smoothed beams of the VULCAN glass laser at the Rutherford Appleton Laboratory were used in a cluster configuration to irradiate a thin high Z layer (0.1μm Au or 0.2μm Bi) which was supported on a thin plastic substrate typically 1μm thick (hereafter the source foil). The laser pulse length was typically 600ps and the focal spot typically 500μm. The soft X-rays emitted through the rear of the target were then used to heat a second, plastic foil (hereafter the sample) which was orientated parallel to the source target and was separated from it by approximately 230μm. The soft X-rays transmitted through the second foil were analysed using a time-resolving XUV spectrometer with spectral and temporal resolutions of approximately 0.2A and 100ps respectively. Absolute time-resolved and time-integrated measurements of broad band spectral fluxes from the rear of the targets were also made using filtered vacuum photodiodes.

3. Modelling

3.1 Radiation Hydrodynamics

The experimental conditions are simulated using a multi-group radiation transport model coupled to the 1D Lagrangian hydrodynamics code MEDUSA.[12] The radiation transport model uses group-averaged Planck mean opacities calculated from a screened-hydrogenic average-atom (AA) calculation which is performed in-line with the hydrodynamics and assumes L.T.E.. This assumption was found to be a good approximation during most of the simulations when a time-dependent AA model based on XSN[13] was used to calculate level occupation probabilities. The behaviour of the source target is not calculated. Instead, the experimentally measured spectrum emitted from the rear of the source foil is used in the calculation to heat the sample.

3.2 Spectral Analysis

For spectral identification and analysis a multi-configuration-Dirac-Fock code is used to calculate atomic physics data (energy levels and oscillator strengths).[14] Configuration abundances for particular plasma conditions are then calculated by solving Saha's equation (i.e. assuming L.T.E.). b-b cross-sections are then calculated according to

$$\sigma(\nu) = (\pi e^2/mc)\ f\ \phi(\nu)$$

where f is the oscillator strength for the transition and ϕ is the line shape function. A radiative transfer algorithm is currently being developed for the prediction of absorption spectra.

4. Experimental Results

4.1 Photodiode Measurements

Measurements were made on bismuth layers 2000A thick deposited on 1 μm plastic substrates for laser irradiances between 1 and 5 10^{14} Wcm^{-2}

with a time-resolving XUV photodiode. The diode was positioned at an angle of 50° to the target normal. It was found that the soft X-ray pulse emitted to the rear of the target closely followed the laser pulse. In addition, a preliminary analysis suggests a conversion efficiency in the backward direction of approximately 7.5 $\pm$2% with no obvious dependence on the laser irradiance in the experimental range. This figure was obtained assuming a radiation field isotropic in the half plane at the rear of the target. The $\pm$2% is to account for the scatter in the data. This conversion efficiency corresponds to effective radiation temperatures in the range of 100-130 eV at the rear of the target. These values are in reasonable agreement with time integrated diode measurements taken at the same time and with other diode measurements taken under similar laser conditions without the use of RPP smoothing where a value of around 12% was found.[15,16] It should be noted that the 7.5% figure is determined as a fraction of the total laser energy delivered by the laser and does not take into account any losses due to diffraction from the phase plates.

It was found that the high Z layer thickness had a significant effect on the soft X-ray conversion efficiency. Measurements were made on targets with three different thicknesses of gold deposited on 1μm CH substrates. While the conversion efficiencies for 1000A thick gold layers were similar to those for bismuth with the same ρr at 7.5%, the value for thinner 500A targets increased to around 12% while that for thicker 2000A targets decreased to less than 4%. This is believed to be due to incomplete burnthrough of the Au layer as ρr is increased.

The target design used for the source foil was 2000A bismuth on 1μm CH. Although this did not produce the best conversion efficiency to soft X-rays, mass ablation rate measurements strongly suggest that the targets would not burn through during the laser pulse. This is supported by the increase in the conversion efficiency with thinner high Z layers. This should ensure that the sample foil was heated only by soft X-rays. Laser light transmission was not measured in these experiments and should be investigated for future work so that source target design can be optimised.

4.2 XUV Spectra

Figure 1 shows time-resolved XUV spectra observed for several different thicknesses of CH sample foil. The most noticeable features in the spectra are the sharp edge feature at around 45A, clear absorption structure below 45A particularly for the thinner foils and shifts of the edge feature towards shorter wavelength (higher energy) with time (by about 5-10eV) also for the thinner foils. For the 6μm sample, there appears to be no noticeable shifting of the edge feature with time. However, comparison with a reference spectrum filtered with a cold 2μm thick CH filter shows that the feature for the 6μm target is shifted by about 5-10eV to the red side of the cold edge position. The cold edge position corresponds very closely to that observed for the edge feature in the reference spectrum except at early times and is expected to be due largely to the instrumental filters which protect the mirrors and grating. The optical depth of the sample foils can be calculated as a function of time from the ratio of the observed spectrum to the reference spectrum. This process is currently underway. Here, initial estimates of the jump ratio (defined as the ratio of the intensity on the low energy side of the edge to that on the high energy side) at the edge feature are given so that effects due to the samples can be assessed.

For the source foil, the jump ratio is approximately 7 at early times and has reduced to 4-5 by the peak of the pulse. The values found when a sample foil is used are generally larger. A value of around 10 is found for a 1μm target for most of the time. This value decreases towards approximately 5 well after the peak of the pulse. In contrast, for a 3μm foil, the ratio is measured to be around 20 at early times, decreasing to 10-15 at later time. Because of the low signal for the 6μm case, a lower limit for the jump ratio of greater than 15-20 only could be measured. Therefore, it is clear that the presence of the sample foil has a direct effect on the jump ratio near the edge feature.

5. Discussion

The heating of a sample can be described as follows. The soft X-rays from the source are initially incident on the cold target material and are absorbed close to the surface over a distance of approximately a photon mean free path and a temperature gradient develops. As the foil becomes heated, preferentially at the front, it ionizes and becomes less opaque to the incident radiation which then propagates further into the target where it is absorbed in the cooler more opaque regions. The photon mean free path is a strong function of plasma conditions and photon energy so that the spectrum of the heating radiation is also important. In addition, we have found that in these circumstances the absorption of radiation emitted in the foil contributes significantly to the foil heating. Figure 2 shows predicted temperature profiles near the peak of the radiation pulse for 1μm and 6μm CH targets for an X-ray conversion efficiency from the source foil typical of the values measured by the photodiodes and corresponding to a radiation temperature of 100eV at the sample. It

is clear that the observed spectrum will be representative of a range of plasma conditions which will depend at least partly on the foil thickness.

It has been shown previously that while the overall features of the observed spectra are reproduced fairly well by the simulations, the small blue shift of the edge feature of just a few eV is not predicted.[9] The possible explanations for this are discussed below.

It is possible that the foil heating is considerably overestimated either due to an exaggeration of the flux from the source foil or to the treatment of the radiation hydrodynamics and that the edge feature is due to a bound-free (b-f) absorption edge resulting from partially ionized carbon ions. Figure 3 shows the approximate positions of b-f edges for all carbon ions in their ground states taking into account continuum lowering using the Stewart-Pyatt approximation.[17] The ionization energies were calculated from the MCDF code. The horizontal bars result from the range of continuum lowering calculated for plasma densities typical of those predicted to exist in the foils near the peak of the pulse (0.1-0.01 g/cc). For b-f absorption to be important in the spectra in the region of the experimentally observed edge feature, a significant fraction of the plasma would have to exist as neutral atoms and/or singly ionized ions since the b-f absorption features of all other ions are expected to exist at wavelengths below about 40A. The fraction of the plasma ions in a neutral or singly ionized state, necessary to produce the observed jump ratios of around 2-4 (found after taking into account the reference spectrum) can be estimated as follows. Approximately 0.1μm of cold material at solid density is required to produce a jump ratio of 2. Therefore, the fraction, f, of a sample foil, of initial thickness rμm at solid density, required to exist as neutral atoms or singly ionized ions to produce this jump ratio is approximately $f \sim 0.1/r$. Figure 4 shows carbon ion fraction calculated as a function of temperature using the Saha equation for a density of 0.01g/cc, a typical value for a 1μm sample near the peak of the pulse . For a 1μm foil $f \sim 0.1$, which, according to figure 4, can only be achieved for temperatures below about 10eV. Indeed, for the predicted temperatures of around 50eV the only significant b-f absorption features are predicted to be due to He- and H-like ions which exist at wavelengths below 35A. Therefore, for photoionization to be a viable explanation of the observed spectral characteristics of the thinner foils, the plasma heating would have to be overestimated in the modelling to a gross extent and this explanation is then made to seem very unlikely.

This is not necessarily the case for the thicker 6μm foil particularly at early time when a significant portion of the foil remains unheated (< 10eV) and in which larger temperature gradients exist. The small, approximately constant, red shift of the edge would then presumably be due to continuum lowering. However, considering the range of plasma conditions predicted to exist during the interaction, it would be surprising if an approximately constant red-shift resulted. Therefore, although from figures 2, 3 and 4 it is clear that b-f absorption in the region of the experimentally observed edge feature will be important, it is not expected to account for the small, approximately constant, red-shift.

Hitherto, we have not considered the effect of bound-bound (b-b) transitions on the spectra. Because of the large b-b cross-sections, absorption features due to b-b transitions of even the less abundant ion species and configurations in the plasma will be important and strong transitions will be observed over a large range of plasma conditions. This will be particularly important for the thicker foils used in the experiment not only because of the larger temperature gradients expected to exist but also because of the large optical depth. Figure 5 shows gf values of some 1s->np transitions between 30 and 45A calculated using the MCDF code for carbon ions. A significant number of transitions exist in the region of the cold carbon K-edge. Figure 6 shows traces taken across wavelength at three different times from a spectrum obtained from a source target (0.1μm Au on 1μm CH) when no sample target was present. (This data was obtained using a higher magnification streak camera than that of figure 1). The approximate positions of some of the 1s-2p and 1s-3p transitions are marked demonstrating evidence of absorption features due to at least He- and H-like carbon ions in the plastic support, consistent with figures 2 and 4. Absorption from less highly ionized species will become more important when samples are used since these must attain lower temperatures than the plastic support of the source target. Although more detailed predictions of the effect of b-b transitions on the absorption spectra require a detailed radiative transfer calculation for the target conditions and gradients, it is clear from figures 5 and 6 that b-b absorption is important in the spectral region just above (in energy) the observed edge feature. In addition, because of the comparatively low temperatures and high densities ($T \lesssim 30$eV, $\rho \sim 0.1$g/cc) predicted to exist towards the rear of the 6μm targets, b-b absorption due to significant fractions of neutral atoms and/or singly ionized ions may contribute substantially to the approximately constant red-shift of the observed edge feature and to the small blue-shift of the edge

STREAK RECORDS OF XUV BISMUTH SPECTRA TRANSMITTED THROUGH PLASTIC FOILS OF DIFFERENT THICKNESSES

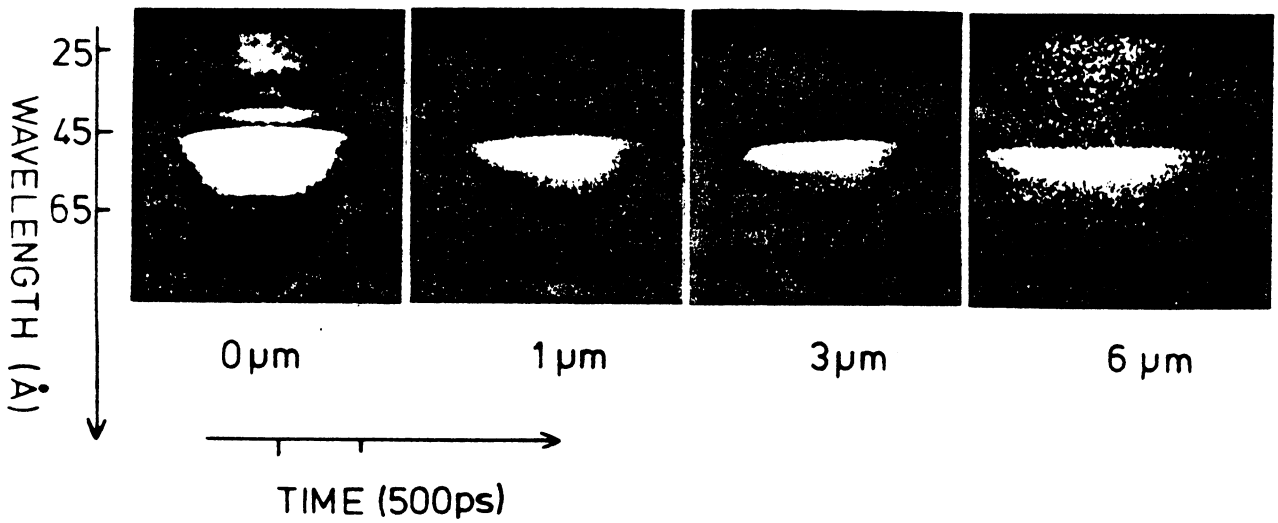

Figure 1. XUV streak data for radiatively heated CH foils.

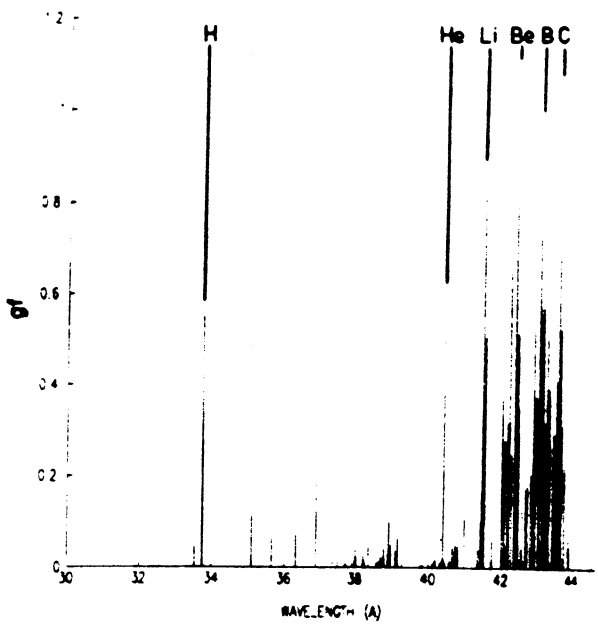

Figure 5. gf values vs wavelength for 1s-np transitions of carbon ions. 1s-2p transitions are marked by ion stage.

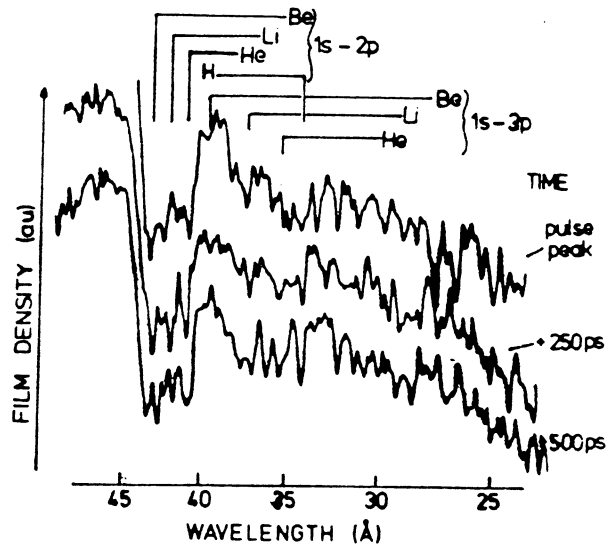

Figure 6. Traces taken across streak data from a source target.

observed for the thinner foils as they become heated and ionized. The calculated wavelengths of these transitions are shown in figure 5 and are very close to the wavelength of the cold carbon K-edge reported in the literature, 43.7A.

6. Conclusions

Radiation transport through radiatively heated plastic foils has been investigated using time-resolved XUV spectroscopy in the sub-KeV energy region. The experimental conditions were simulated with a multi-group radiation hydrodynamics code and global features of the observed spectra were reproduced fairly well by the modelling. However, the small blue-shift with time of the observed edge feature for thinner foils and the approximately constant red-shift of the feature for a 6μm sample were not predicted. It is expected that this is largely due to the omission of b-b transitions in the modelling. Future experiments must include direct measurements of target gradients and conditions so that our ability to model the energy transport in the samples and to predict spectra under these conditions can be better assessed.

References

1. D.G. Colombant et al., Phys. Fluids, **18**, 1687, (1975).
2. R.W. Lee, J.Q.S.R.T., **27**, 87, (1982).
3. R.W. Lee, J.Q.S.R.T., **27**, 243, (1982).
4. D. Duston et al., Phys. Rev. **A27**, 1441, (1983).
5. D. Duston et al., Phys. Rev. **A31**, 3220, (1985).
6. T. Mochizuki et al., Phys. Rev. **A36**, 3279, (1987).
7. J.M. Salter et al., J.Q.S.R.T., **39**, 139, (1988).
8. C. Chenais-Popovics et al., Phys. Rev. **A40**, 3194, (1989).
9. J. Edwards et al., Europhys. Lett., **11**, 631, (1990).
10. R. Sigel et al., P.R.L., **65**, 587, (1990).
11. J. Bruneau et al., P.R.L., **65**, 1435,(1990).
12. J.P. Christiansen et al., Comp. Phys. Commun., **7**, (1974).
13. W.A. Lokke and W.H. Grasberger, LLNL report, UCRL-52276, (1977).
14. I.P. Grant et al., Comp. Phys. Commun., **21**, 207, (1980). B.J. McKenzie et al., Comp. Phys. Commun., **21**, 233, (1980).
15. C.A. Back et al. these proceedings.
16. S.J Davidson Priv. comm.
17. J. Stewart and K. Pyatt, Astrophys. J., **144**, 1203, (1966).

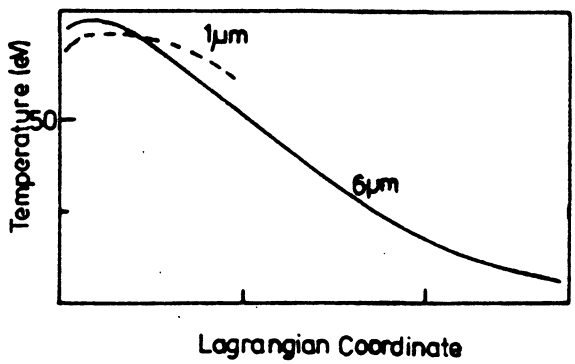

Figure 2. Predicted temperature profiles for 1μm and 6μm targets.

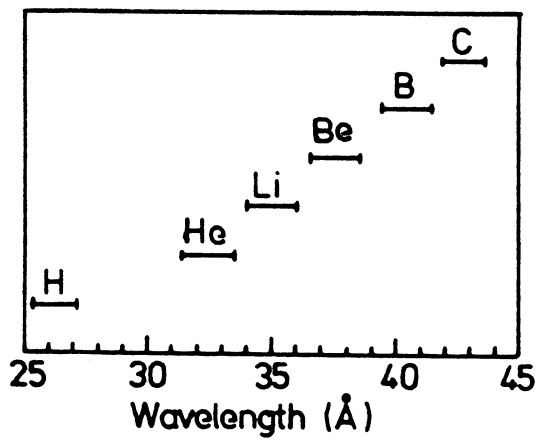

Figure 3. b-f edge wavelengths for carbon ions.

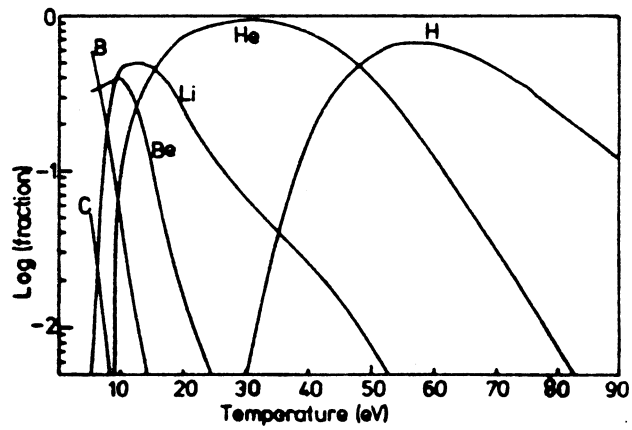

Figure 4. Carbon ion fractions vs temperature at 0.01 g/cc.